Cloete, Schalk; Ruhnau, Oliver; Cloete, Jan Hendrik; Hirth, Lion

Working Paper

Blue hydrogen and industrial base products: The future of fossil fuel exporters in a net-zero world

Supplementary material to

Blue hydrogen and industrial base products: The future of fossil fuel exporters in a net-zero world

Schalk Cloete [a], Oliver Ruhnau [b], Jan Hendrik Cloete [c], and Lion Hirth [b,c,d]*

[a] SINTEF Industry, Trondheim, Norway

[b] Hertie School of Governance, Berlin

[c] Neon Neue Energieökonomik GmbH

[d] Mercator Research Institute on Global Commons and Climate Change (MCC)

*Corresponding author

Flow Technology Group, SINTEF Industry

S.P. Andersens vei 15B, 7031 Trondheim, Norway

Email: schalk.cloete@sintef.no

Nomenclature

Symbols:

α	Hourly availability (fraction)
γ	CO_2 capture rate (ton/MWh)
δ	Load (MW or tph)
η	Conversion efficiency (%)
ι	Import rate (MW or tph)
λ	Technology lifetime (years)
C	Total system cost (€)
c^{fix}	Fixed cost (€/MW/year, €/tph/year, €/MWh/year, €/MW/km/year, or €/tph/km/year)
c^{var}	Variable cost (€/MWh or €/ton)
d	Link length (km)
f	Inflow rate of water to hydropower reservoirs (MW)
G	Total annual generation (MWh)
g	Generation/production (MW or tph)
$\hat{g}$	Generation/production capacity (MW or tph)
$\hat{n}$	Link capacity (MW or tph)
p	Product price (€/MWh or €/ton)
r	Discount rate (%)
s	CO_2 storage rate (tph)
v	Volume of stored energy (MWh)
$\hat{v}$	Storage volume (MWh)

Sub- and superscripts:

bat	Battery
cap	Capital
el	Electric
GERN	North Germany
GERS	South Germany
$\mathrm{H2CC}$	Hydrogen combined cycle
$\mathrm{H2GT}$	Hydrogen gas turbine
hydro	Reservoir hydropower
i	Index for generating technologies
$i_{\mathrm{CO_2}}$	Index for generating technologies that consume natural gas
i_{gen}	Index for all electricity generating technologies
i_{NG}	Index for generating technologies that consume natural gas
i_{RE}	Index for renewable generating technologies
j	Index for storage technologies
k	Index for link technologies
l	Index for links between different nodes
n	Index for nodes
n_{GER}	Index for German nodes
NG	Natural gas
NOR	Norway
p	Index for different products

pump Pumped hydro
salt Salt caverns

Model equations

The objective of the model is to minimize total system costs by optimizing deployment and dispatch as follows:

- Deployment of electricity, hydrogen, and steel producers $(\hat{g})$, electricity and hydrogen storage $(\hat{v})$, and inter-node transmission networks for electricity, hydrogen, and CO_2 $(\hat{n})$ spanning given distances (d)
- Hourly power, hydrogen, and steel production, consumption, charging, and discharging (g) from each production technology
- Natural gas production $\left(g^{\mathrm{NG}}\right)$ and CO_2 storage $\left(s^{\mathrm{CO_2}}\right)$
- Hourly imports of natural gas, steel, and ammonia (ι^p) from the global market

Total system costs are depicted in Equation 1. From left to right, the terms on the right-hand side represent: annualized capital costs and fixed operating and maintenance (O&M) costs for generators (i), storage technologies (j) and transmission technologies (k) over all nodes (n) and inter-node links (l) included in the simulation; non-fuel variable O&M costs summed over all relevant generating technologies, nodes, and timesteps (t); natural gas production and CO_2 storage at costs of p^{NG} and p^{CO_2}, respectively; world market imports of various products (p), i.e., natural gas, steel, and ammonia, at their respective exogenously specified prices (p^p), noting that exports are negative imports with lower prices.

$$C = \sum_{i,n} c_i^{\mathrm{fix}} \hat{g}_{i,n} + \sum_{j,n} c_j^{\mathrm{fix}} \hat{v}_{j,n} + \sum_{k,l} c_k^{\mathrm{fix}} \hat{n}_{k,l} d_{k,l} + \sum_{t,i,n} c_i^{\mathrm{var}} g_{t,i,n} + \sum_{t,n} g_{t,n}^{\mathrm{NG}} p^{\mathrm{NG}} + \sum_{t,n} s_{t,n}^{\mathrm{CO_2}} p^{\mathrm{CO_2}} + \sum_{t,n,p} \iota_{t,n}^{p} p^{p} \qquad \textit{Equation 1}$$

Fixed costs are composed of annualized capital costs $\left(c^{\mathrm{fix,cap}}\right)$ and fixed O&M costs. To account for the time-value of money, capital costs (c^{cap}) are annualized using an assumed lifetime (λ) for each technology and a given discount rate (r).

$$c^{\mathrm{fix,cap}} = \frac{c^{\mathrm{cap}} r (1+r)^{\lambda}}{(1+r)^{\lambda} - 1} \qquad \textit{Equation 2}$$

Five balances are solved for the five commodities in each node. Electricity generation (g with $p = \mathrm{el}$ in Equation 3) includes power production from all generating technologies and battery discharge, as well as electricity consumption (negative generation) from PEM, battery and pumped hydro charging, GSR hydrogen production, steel production, and reconversion plants for imported ammonia. The load (δ) in each timestep in each node must be met by the sum of generation and imports (via the modelled HVDC links) from other nodes.

$$\delta_{t,n}^{\mathrm{el}} = \sum_{i} g_{t,i,n}^{\mathrm{el}} + \iota_{t,n}^{\mathrm{el}} \qquad \forall\, t,n$$ *Equation 3*

The hydrogen balance is similar with the addition of a possibility for ammonia imports (η^{NH_3} is the efficiency with which ammonia is converted back into hydrogen). The first term on the right-hand side includes hydrogen production from various technologies, negative inflows and positive outflows from hydrogen storage, as well as consumption (negative generation) from steel production. The final bracketed term represents the consumption from hydrogen-fired power plants.

$$\delta_{t,n}^{\mathrm{H_2}} = \sum_{i} g_{t,i,n}^{\mathrm{H_2}} + \iota_{t,n}^{\mathrm{H_2}} + \iota_{t,n}^{\mathrm{NH_3}} \eta^{\mathrm{NH_3}} - \left(\frac{g_{t,n,\mathrm{H2CC}}}{\eta_{\mathrm{H2CC}}} + \frac{g_{t,n,\mathrm{H2GT}}}{\eta_{\mathrm{H2GT}}} \right) \qquad \forall\, t,n$$ *Equation 4*

For natural gas, the balance includes all electricity and hydrogen generating technologies that consume natural gas as well as natural gas imports. An additional distinction is that natural gas demand is endogenously determined, as opposed to the exogenous specification for hydrogen and electricity. Here, i_{NG} is an index for all the technologies that require natural gas as an input and $\eta_{i_{\mathrm{NG}}}$ is the conversion efficiency of natural gas into products using those technologies.

$$g_{t,n}^{\mathrm{NG}} = \sum_{i_{\mathrm{NG}}} \frac{g_{t,i_{\mathrm{NG}},n}}{\eta_{i_{\mathrm{NG}}}} + \iota_{t,n}^{\mathrm{NG}} \qquad \forall\, t,n$$ *Equation 5*

For Germany, $g_t^{NG} = 0$, meaning that all natural gas consumption must be balanced by imports. On the other hand, Norwegian natural gas production cannot exceed a specified maximum annual limit, G. This also implies that Norway cannot import natural gas.

$$\sum_{t} g_{NOR}^{NG} \leq G_{NOR}^{NG}$$ *Equation 6*

The CO_2 balance involves all technologies that capture CO_2 as designated by the index $i_{\mathrm{CO_2}}$. Pipeline flows between nodes is also included. Like the natural gas balance, the demand for CO_2 storage is endogenous. In addition, it is set to zero in the German nodes, forcing Germany to export any captured CO_2 to Norway for storage. Here, $\gamma^{p_{NG}}$ is the amount of CO_2 captured per unit energy produced.

$$s_{t,n}^{\mathrm{CO_2}} = \sum_{i_{\mathrm{CO_2}}} g_{t,i_{\mathrm{CO_2}},n} \gamma_{i_{\mathrm{CO_2}}} + \iota_{t,n}^{\mathrm{CO_2}} \qquad \forall\, t,n$$ *Equation 7*

Lastly, the steel balance satisfies the exogenously specified steel demand in each node using net production (the H_2-DRI process and storage) and imports. Steel storage is assumed to be free.

$$\delta_{t,n}^{\text{steel}} = g_{t,steel,n} + \iota_{t,n}^{\text{steel}} \qquad \forall\, t, n \qquad \textit{Equation 8}$$

For generating technologies, hourly generation is constrained to the maximum available (α) capacity for every hour of the year. For dispatchable generators $\alpha = 1$, given that the availability of modern natural gas plants is essentially 100% (NREL, 2018). Hourly availability profiles are used for run-of-the-river hydro, wind, and solar, as specified in the next section. It is noted that electricity consumers like PEM, battery charging, and pumped hydro are also included, only with negative generation. For GSR, provision is made that the sum of electricity and hydrogen production cannot exceed installed capacity.

$$g_{t,i,n} \leq \alpha_{t,i}\hat{g}_{i,n} \qquad \forall\, t, i, n \qquad \textit{Equation 9}$$

The full year capacity factor of any generating technology cannot exceed 0.9 to reflect the need for plant downtime for routine maintenance.

$$\sum_{t} g_{t,i} \leq 0.9 \cdot 8760 \cdot \hat{g}_i \qquad \forall\, i \qquad \textit{Equation 10}$$

For energy storage, the installed storage volume is another important constraint, where the total volume of stored electricity (v) cannot exceed the installed energy storage capacity $(\hat{v})$. For salt caverns, the stored volume cannot exceed half the installed capacity due to the need to keep storage volumes between 30 and 80% (Walker et al., 2018). Maximum hydro storage volume is also constrained to reflect geographical limits.

$$v_{t,j,n} \leq \hat{v}_{j,n} \qquad \forall\, t, j, n \qquad \textit{Equation 11}$$

The evolution of stored energy over time for batteries, pumped hydro, and hydrogen is shown below. Each equation is constrained so that the stored energy must be identical in the first and last timesteps of the year. In Equation 13, f is the hourly inflow into hydropower reservoirs. For hydrogen storage (Equation 14 and Equation 15), g^{H_2} is the rate of storage charge (negative) or discharge (positive) viewed as a hydrogen generating technology in the hydrogen energy balance (Equation 4).

$$v_{t,n,\text{bat}} = v_{t-1,n,\text{bat}} - \left(g_{t,n,\text{bat}}^{\text{in}} + \frac{g_{t,n,\text{bat}}^{\text{out}}}{\eta_{\text{bat}}} \right) \qquad \forall\, t, n \qquad \textit{Equation 12}$$

$$v_{t,\text{hydro},n} = v_{t-1,\text{hydro},n} - \left(g_{t,\text{hydro},n} + g_{t,n,\text{pump}} \cdot \eta_{\text{pump}} \right) + f_{t,n} \qquad \forall\, t, n \qquad \textit{Equation 13}$$

$$v_{t,\text{salt},n} = v_{t-1,\text{salt},n} - g_{t,\text{salt},n}^{H_2} \qquad \forall\, t, n \qquad \textit{Equation 14}$$

$$v_{t,\text{tank},n} = v_{t-1,\text{tank},n} - g^{H_2}_{t,\text{tank},n} \qquad \forall\, t, n \qquad \textit{Equation 15}$$

For salt caverns, the need for added hydrogen transmission capacity ($\hat{g}_{\text{salt}}$) to reach these geographically constrained sites and the charge/discharge limit of 10%/day are included as follows. Also, salt caverns are only allowed in Norway and North Germany.

$$\text{abs}\left(v_{t,\text{salt},n} - v_{t-1,\text{salt},n}\right) \leq \hat{g}_{\text{salt},n} \qquad \forall\, t, n \qquad \textit{Equation 16}$$

$$\hat{g}_{\text{salt},n} = \frac{0.1 \cdot \hat{v}_{\text{salt},n}}{24} \qquad \forall\, n \qquad \textit{Equation 17}$$

Flows of electricity, hydrogen, and CO_2 between the three nodes are described by relating the net import balance of each node to the flows through the links between them. In this case, the net import balances for Norway, North Germany, and South Germany are specified as follows:

$$\iota^{p}_{t,\text{NOR}} = -n^{p}_{t,\text{NOR}-\text{GERN}} \qquad \forall\, t, p \qquad \textit{Equation 18}$$

$$\iota^{p}_{t,\text{GERN}} = n^{p}_{t,\text{NOR}-\text{GERN}} - n^{p}_{t,\text{GERN}-\text{GERS}} \qquad \forall\, t, p \qquad \textit{Equation 19}$$

$$\iota^{p}_{t,\text{GERS}} = n^{p}_{t,\text{GERN}-\text{GERS}} \qquad \forall\, t, p \qquad \textit{Equation 20}$$

The maximum flow of any product through the links cannot exceed the installed capacity:

$$n^{p}_{t,l} \leq \hat{n}^{p}_{l} \qquad \forall\, t, l, p \qquad \textit{Equation 21}$$

Finally, several limits can be imposed in the model. Equation 22 shows the limit imposed on the amount of renewable energy capacity that can be constructed in each node. For Germany, Equation 23 enforces a minimum renewable energy share in electricity generation of 80%. A similar limit is imposed at 95% for Norway (Equation 24). Lastly, net exports of electricity or hydrogen from Norway can be set to zero using Equation 25 to enhance energy security, still allowing for flows to balance supply and demand that sum to zero across the year.

$$\hat{g}_{i_{\text{RE}},n} \leq \hat{g}^{\text{limit}}_{i_{\text{RE}},n} \qquad \forall\, i, n \qquad \textit{Equation 22}$$

$$\sum_{t,i_{\text{RE}},n_{\text{GER}}} g_{t,i_{\text{RE}},n_{\text{GER}}} \geq 0.8 \sum_{t,i_{\text{gen}},n_{GER}} g_{t,i_{\text{gen}},n_{\text{GER}}} \qquad \forall\, t, i, n \qquad \textit{Equation 23}$$

$$\sum_{t,i_{\text{RE}}} g_{t,i_{\text{RE}},\text{NOR}} \geq 0.95 \sum_{t,i_{\text{gen}}} g_{t,i_{\text{gen}},\text{NOR}} \qquad \forall\, t, i \qquad \textit{Equation 24}$$

$$\sum_{t} n^{p}_{t,\mathrm{NOR-GERN}} = 0 \qquad \forall\, p$$ *Equation 25*

Technology cost and performance

The main technology assumptions employed in this study are summarized in Table S1 to Table S4. These numbers are selected to be representative of 2040.

In Table S1, three efficiencies are indicated for the flexible GSR technology: a net electric efficiency (El), a hydrogen production efficiency (H_2), and an electric efficiency in hydrogen production mode (El H_2). The latter is negative, indicating that GSR consumes some power when producing hydrogen. The costs of both GSR plants (GSR and GSRH2) were scaled up from original studies (Nazir et al., 2020; Szima et al., 2019) to the standards of the IEA (IEA, 2019a, 2020) by keeping the same ratio between the costs of plants with CO_2 capture and reference plants without capture. It is also noted that the efficiency of all gas-fired power plants are reduced by 2 %-points relative to our previous study (Cloete et al., 2021) because these plants will only be used for supplying the residual load, with frequent ramping and part-load operation reducing average efficiency.

For simplicity, VRE transmission costs are included directly in the capital costs of hydro, wind, and solar plants to account for their non-ideal spatial correlation with demand. Costs are roughly approximated from a review (Gorman et al., 2019) that reported median transmission costs of 350 $/kW for wind from 40 studies and 266 $/kW for solar from 15 studies. These numbers are associated with high uncertainty as indicated by the wide ranges in the referenced review (Gorman et al., 2019). It is noted that the transmission costs assumed in Table S1 are lower than these numbers because transmission lines would typically be annualized using a longer lifetime than that assumed for the different generating technologies. Hydro and offshore wind are assigned higher transmission costs because these technologies face stronger geographical constraints than onshore wind and solar PV.

Table S1: Summary of technology assumptions for electricity and hydrogen generators. Costs were converted using an exchange rate of 1.2 $/€ where necessary.

Technology	Capital cost (€/kW)	Efficiency (%)	Lifetime (years)	Fixed O&M (%/year)	Variable O&M (€/MWh)	CO_2 avoidance (%)	Ref.
Run-of-the-river hydro + transmission	1370 + 300	-	40	2	-	-	(NVE, 2020)
Reservoir hydro + transmission	1560 + 300	-	40	2	-	-	(NVE, 2020)
NGCC with CCS	1300	56	40	2.5	4	90	(Cloete et al., 2021)
NGCC	833	63	40	2.5	2	-	(IEA, 2020)

H2CC	833	63	40	2.5	2	-	(Cloete et al., 2021)
GSR	1392	56 (El), 84 (H_2), -5 (El H_2)	40	2.5	4	98	(Cloete et al., 2021)
OCGT	467	43	30	2.5	2	-	(Cloete et al., 2021)
H2GT	467	43	30	2.5	2	-	(Cloete et al., 2021)
Onshore wind + transmission	1150 + 200	-	25	2	-	-	(IEA, 2020)
Offshore wind + offshore transmission + onshore transmission	1250 + 500 + 300	-	25	2	-	-	(IEA, 2019b)
Solar PV + transmission	367 + 150	-	25	2	-	-	(IEA, 2020)
Electrolysis - transmission avoidance + H_2 transmission	375 - 250 + 100	72	25	2	-		(IEA, 2019a)
SMR with CCS	1067	69	40	3	2	90	(IEA, 2019a)
GSRH2	860	87 (H_2), -5 (El H_2)	40	3	2	97	(Nazir et al., 2020)
NH_3 reconversion	433	99 (H_2), -4.5 (El)	40	3	-	-	(IEA, 2019a)

Wind and solar time series are taken from Renewables Ninja (Pfenninger and Staffell, 2016; Staffell and Pfenninger, 2016) and load profiles from the Open Power System Data project (Neon, 2020), all for the year 2017. For Germany, the data is split between North and South based on federal states as depicted in Figure S1. In general, federal states with high wind resources are assigned to the Northern node, while those with high load are assigned to the southern node. Wind and solar profiles are retrieved on the NUTS-2 level and averaged within the two zones. On the demand side, the national load profile is split into North and South with a 1:2 ratio (LAK, 2021).

Table S2 summarizes assumptions regarding capacity factors and limits. Onshore and offshore wind profiles are adjusted using a second order polynomial between 0 and 1 to achieve higher capacity

factors with future technology gains, whereas solar profiles are left unchanged. For onshore wind, North Germany is assigned a capacity factor of 30% as projected by the IEA for Europe (IEA, 2020), whereas South Germany is scaled proportionately to North Germany. Norway is given a higher capacity factor of 37% according to current performance (EFN, 2021). These numbers represent large performance increases of around 50% relative to the original time series from Renewables Ninja. Capacity limits are set to 1.5% of available land in Germany in light of expansion delays in recent years that draws into question the commonly assumed 2% number. A stricter limit is imposed in Norway due to strong public resistance.

Figure S1: Assumed split between the German North and South nodes.

Offshore wind capacity factors for Germany will be increasingly constrained at higher installed capacities due to wake effects (Agora, 2020), resulting in capacity factors of around 38% for 50 GW of installed capacity and 30% for 100 GW. Thus, 50 GW was selected as an approximate point where more offshore wind would become uneconomical. Such data is not available for Norway, but offshore wind expansions should face less performance reduction with more installed capacity due to Norway's larger coastline. However, all Norwegian offshore resources will be in deep water, potentially requiring floating turbines with somewhat reduced performance relative to fixed turbines. Thus, the Norwegian offshore wind capacity factor was left unchanged from Renewable Ninja numbers at 50%.

Table S2: Assumed capacity factors and capacity limits for the three nodes considered in the study.

	Norway	North Germany	South Germany
Onshore wind	37% & 20 GW	30% & 63 GW	21.4% & 75 GW
Offshore wind	50% & 50 GW	40% & 50 GW	
Solar PV	10.5% & 200 GW	12.9% & 200 GW	13.3% & 300 GW
Run-of-the-river hydro	33.1% & 14 GW		100% & 2.3 GW

Norwegian hydropower inflow profiles (Amundsen and Bergman, 2006) are considered to charge the reservoirs and represent the generation profile for run-of-the-river plants. A small run-of-the-river

potential in South Germany is assumed to generate constantly at 100% capacity factor. Capacity limits for Norway are calculated from knowledge that about 75% of Norway's hydropower production is flexible (EFN, 2021) and that the maximum potential is 163.6 TWh/year (Norwegian Ministry of Petroleum and Energy, 2015). German limits are set from the total production of 20.2 TWh in 2017 (BP, 2020). For reservoir hydro in Norway, total annual inflows are set to 75% of the 163.6 TWh/year mentioned earlier with no constraints on the amount of capacity that can be constructed.

Energy storage costs are summarized in Table S3. For pumped hydro, costs are determined by subtracting the cost of reservoir hydro from the cost reported (Mongird et al., 2020) for a standalone pumped hydro facility. Pumped hydro is implemented as a mechanism to increase the stored energy in the reservoir that can be used to generate power using installed reservoir hydro capacity. The power-related cost of salt caverns arises from the H_2 transmission lines required to connect these geographically constrained sites with producers and demand centres. It is noted that only half of installed salt cavern storage is available for practical use (Walker et al., 2018), essentially doubling the cost in Table S3.

Table S3: Summary of technology assumptions for energy storage. Costs were converted using an exchange rate of 1.2 $/€ where necessary.

Technology	Capital cost	Efficiency (%)	Lifetime (years)	Fixed O&M (%/year)	Ref.
Battery power, energy	79 €/kW	86	20	3	(IEA, 2019a)
Battery energy	92 €/kWh		20	10	(IEA, 2019a)
Pumped hydro	640 €/kW	80	40	2	(Mongird et al., 2020)
H_2 cavern power	200 €/kW	100	25	6	(Cloete et al., 2021)
H_2 cavern energy	1 €/kWh		25	3	(Ahluwalia et al., 2019; Walker et al., 2018)
H_2 tank	15 €/kWh	100	25	4	

Cost assumptions related to the transmission of electricity, hydrogen, and CO_2 between the three different nodes in the study are shown in Table S4. Fixed O&M costs are calculated to include the electric losses involved in HVDC cables and converter stations and hydrogen pumping stations. These losses are estimated to be 5% (May et al., 2016) and 3% (Witkowski et al., 2017) of the transported electrical and hydrogen energy, respectively, for a 500 km line. The line length between Norway and North Germany is assumed to be 700 km, while the length between North and South Germany is 500 km.

Table S4: Summary of technology assumptions for energy storage. Costs were converted using an exchange rate of 1.2 $/€ where necessary.

Technology	Capital cost	Lifetime (years)	Fixed O&M (%/year)	Ref.
Electricity (HVDC)	1600 €/MW/km	40	5.3	(Vrana and Härtel, 2018)
Hydrogen	583 €/MW/km	25	7.4	(IEA, 2019a)
CO_2	680 €/(ton/h)	25	2	(IEAGHG, 2011)

The cost of clean steelmaking is taken from (Vogl et al., 2018) where the H_2-DRI process is compared to the conventional blast furnace route. After subtracting electrolyser costs, the remaining costs (shaft furnace and electric arc furnace) amount to 3627 €/(kg/h) with O&M costs equal to 16%/year of this capital cost. Raw material costs (iron ore pellets, fluxes, alloys, and electrodes) amount to €182/ton liquid steel. The additional cost of converting liquid steel to final products was estimated by finding the difference between the levelized liquid steel cost of a conventional blast furnace plant in Europe subject to a €40/ton CO_2 price (€414/ton (Vogl et al., 2018)) and European steel prices (~€460/ton). This difference of €46/ton steel was added to the €182/ton raw material costs. Energy carrier demand per ton of steel includes 1.7 MWh of hydrogen for iron ore reduction in the shaft furnace, 0.75 MWh of electricity for the electric arc furnace and an additional 0.34 MWh of energy to heat the shaft furnace that can be either hydrogen or electricity (Vogl et al., 2018). These hydrogen and electricity requirements must be met via the production, transmission, and storage infrastructure simulated in this study.

Timestep independence

Figure S2 illustrates the sensitivity to shortening simulation times by skipping hours at regular intervals throughout the year. The simulation increased with the cube of the number of simulated hours. For example, whereas the simulation of every 7th hour (as selected for all the cases in the paper) took about 90 minutes per case, the simulation of every 3rd hour required about 900 minutes (impractical for the large number of cases presented).

Fortunately, Figure S2 shows only mild sensitivities to the number of timesteps skipped, especially for finer resolutions than every 7th hour. The amount of Norwegian steel exports showed the greatest variation between cases Figure S2b, given that German steel production was right on the border of being competitive with imports. Small changes in the simulation therefore caused relatively large changes in the German hydrogen demand for steel production.

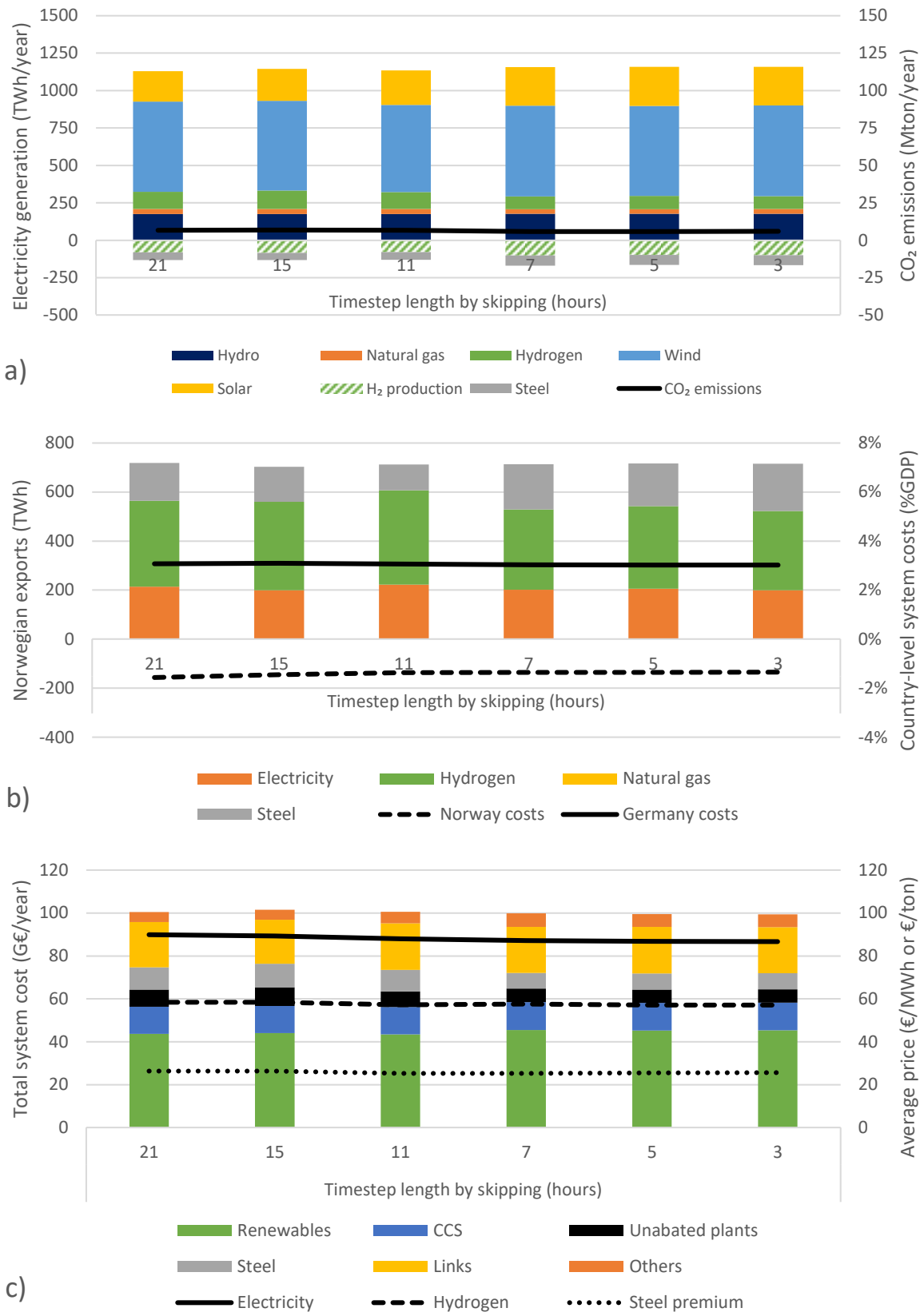

Figure S2: Results from the assessment of different timestep lengths. Electricity generation, emissions, system costs, and commodity prices are aggregated across all three nodes. In panel b, steel trade flows are presented in energy equivalent terms: 2.79 MWh of hydrogen and electricity per ton of steel. In panel c, the steel premium is the difference between German steel prices and the assumed world export price of €470/ton and "Others" include electrolysers, batteries, pumped storage, hydrogen storage, and natural gas export profits.

Furthermore, solar PV production in South Germany increased slightly when the resolution was refined to every 7th hour. At this resolution, daily battery charging cycles could be adequately captured, making solar + batteries more attractive relative to wind, also causing a slight decrease in German electricity prices. However, no significant change in solar deployment was observed at finer resolutions. Thus, simulating every 7th hour was selected as a good balance between accuracy and computational cost for this study.

Sensitivity to technology assumptions

This section presents a sensitivity with optimistic and pessimistic green and blue technology assumptions in the baseline scenario.

Green assumptions:

- The pessimistic scenario investigates greater public resistance: 33% reduction in onshore wind potential (1% of land in Germany), 20% increase in RE transmission costs and a doubling in the cost of HVDC transmission between North and South Germany.
- The optimistic scenario investigates greater public acceptance and green technology cost declines: 33% increase in onshore wind potential (2% of land in Germany) and a 20% decrease in wind, solar, battery, and electrolyser costs.

Blue assumptions:

- The pessimistic scenario assumes that no advanced blue hydrogen technologies like GSR will be commercialized. Only conventional SMR with CCS is available for blue hydrogen production.
- The optimistic scenario reduces GSRH2 plant costs to €500/kW via economies of scale involved in GW-scale plants for blue H_2 exports and the avoidance of H_2 compressors when H_2 is used in steel production. The membrane-assisted autothermal reforming concept (Cloete et al., 2019) is particularly suitable to low-pressure hydrogen production for steelmaking, with hydrogen and electric efficiencies of 94% and -2%, respectively, when producing H_2 at 1 bar. Alternatively, the GSR technology could also be efficiently integrated with a shaft furnace to achieve similar performance, as outlined in the next section. To represent the potential of these processes, the hydrogen and electricity requirements of the H_2-DRI process are reduced by 8% for Norwegian production in this scenario. In addition, enhanced oil recovery is assumed to cancel out the cost of local CO_2 transport and storage in Norway.

Figure S3 shows moderate sensitivities to both sets of assumptions. In the green scenarios, the maximum potential of onshore wind has a limited effect because offshore wind can displace onshore wind at a minor increase in system costs. Transmission system and green technology costs have a larger impact, driving a difference in system costs equivalent to 0.4% of GDP both for Norway and Germany between the pessimistic and optimistic assumptions. In the Green Optimistic scenario, lower wind, solar, battery, and electrolyser costs drive more green hydrogen deployment in Germany, cutting blue hydrogen imports from Norway by 34% (Figure S3b). Electricity imports also reduce by 32%. Norway exports more steel in this scenario, driven by lower blue hydrogen demand from Germany and higher steel export profits (caused by lower green electricity costs for steelmaking) at the fixed export price of €470/ton.

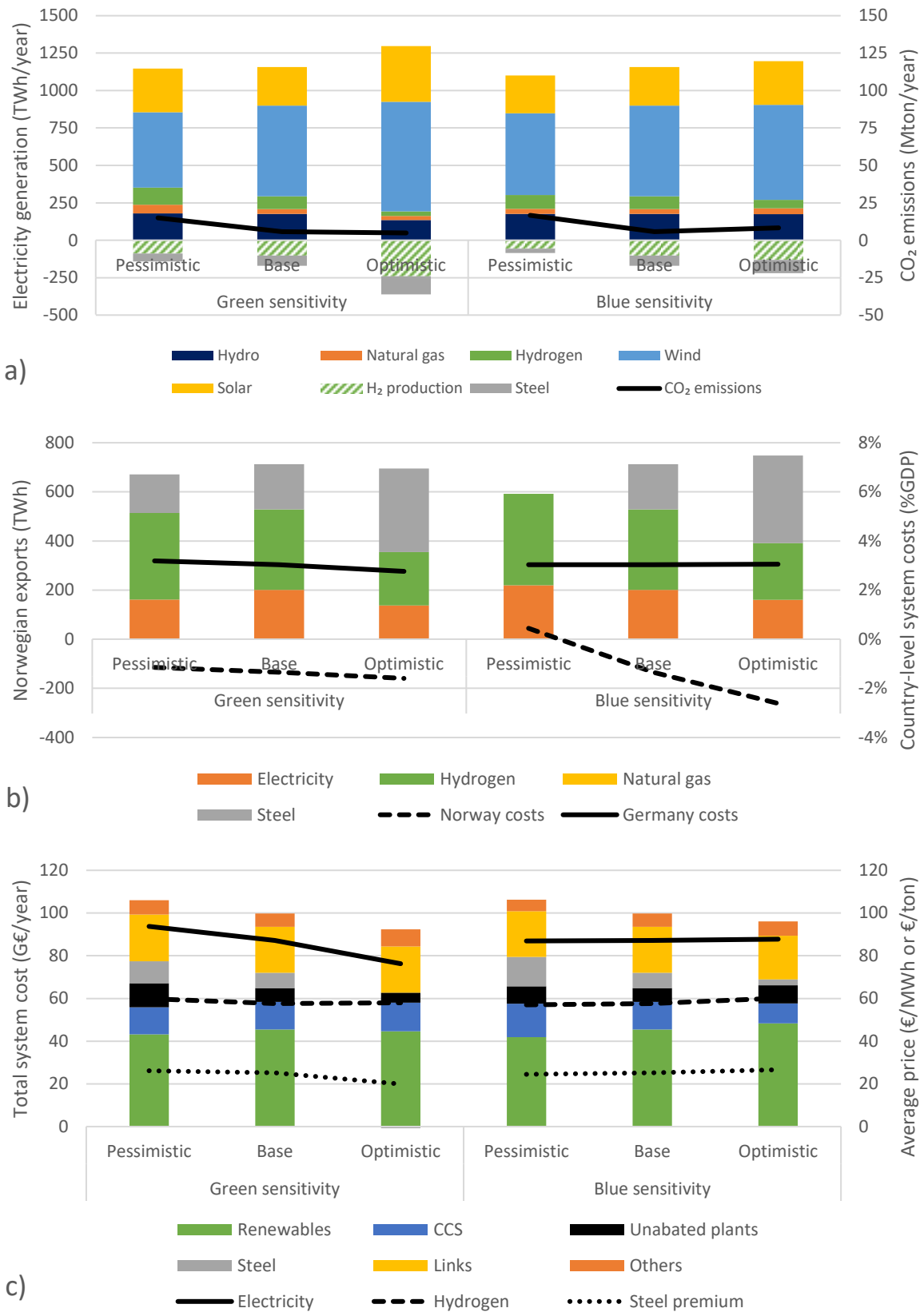

Figure S3: Results from the assessment of different technology assumptions. Electricity generation, emissions, system costs, and commodity prices are aggregated across all three nodes. In panel b, steel trade flows are presented in energy equivalent terms: 2.79 MWh of hydrogen and electricity per ton of steel. In panel c, the steel premium is the difference between German steel prices and the assumed world export price of €470/ton and "Others" include electrolysers, batteries, pumped storage, hydrogen storage, and natural gas export profits.

In the Blue Pessimistic scenario, Figure S3b shows that Norway no longer exports steel. This is due to the lower H_2 production efficiency of SMR-CCS relative to GSRH2 that increases the cost and limits the availability of blue hydrogen. GSRH2 consumes some electricity in exchange for its high H_2 production efficiency, but green electricity supply is not a limiting factor like the natural gas production constraint of 600 TWh/year. In contrast, the Blue Optimistic case strongly increases steel production, driven by the more efficient process integration that reduces energy demand. In terms of costs, blue technology assumptions have an insignificant effect on Germany, but a large effect Norway: The difference between optimistic and pessimistic assumptions amounts to 3.1% of Norwegian GDP (€11 billion). Norway therefore has a strong incentive to maximize the technological potential of blue hydrogen.

Cost evaluation of low-carbon steelmaking technologies

To assess whether blue H_2-DRI steel produced in Norway will be able to compete with coal-based steel produced in developing countries (e.g., India and China), the cost of several such technologies are compared in Figure S4 against the steel market price considered in this paper, as a function of the CO_2 price. The costs were calculated based on the costs and CO_2 intensities reported in the study of Kuramochi et al. (2012).

The conventional integrated steelmaking process based on blast furnaces is severely impacted by rising CO_2 taxes and becomes uncompetitive even at relatively low CO_2 prices. Applying CCS to the integrated steelmaking process is challenging due to numerous emission points with relatively low CO_2 concentrations. The best route for CCS is by implementing top gas recycling (TGR), where CO_2 is captured from blast furnace off-gas and the CO is re-used in the furnace. However, only about half the CO_2 is avoided in this case and the production cost rapidly rises to uneconomical values with increasing CO_2 price. It may be noted that at the high CO_2 prices considered here, it would likely be economical to also capture CO_2 from smaller and more dilute sources in the integrated steelmaking process, rather than only from the blast furnace as considered by Kuramochi et al. (2012), thereby further lowering the CO_2 intensity of the produced steel. However, CO_2 capture gets increasingly costly with more dilute and smaller CO_2 streams, so the blast furnace will remain uncompetitive in a net-zero world.

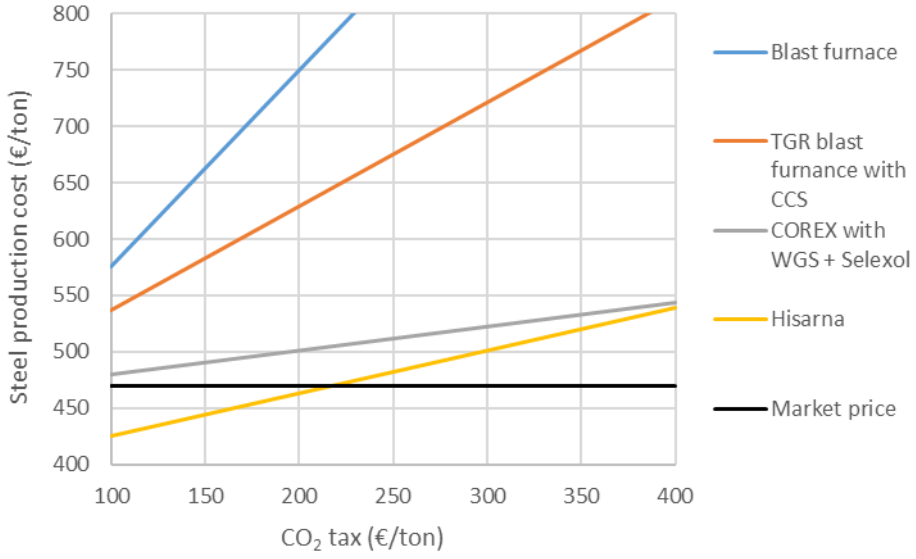

Figure S4: Comparison of the cost of steel production from various coal-based processes as a function of the CO_2 tax price compared to the export price of €470/ton assumed as the base case in the present study.

Smelting reduction steelmaking technologies are typically more suitable to CCS, due to higher CO_2 concentrations and fewer emission points. From Figure S4, both the COREX process (applying a water-gas shift (WGS) and Selexol CO_2 capture) and the advanced smelting reduction process, HIsarna, returns more competitive steel prices. The low cost of the HIsarna process is a result of process characteristics that allows iron ores and non-coking coal to be directly charged to the smelter and the fact that the process produces 85% of the CO_2 from a single stack without nitrogen dilution, making it ideally suitable for CO_2 capture. From the results of (Kuramochi et al., 2012), the HIsarna process has a higher CO_2 intensity than the COREX process with CCS considered here, resulting in a smaller gap in the costs of these two options as the CO_2 tax increases. However, it can be noted that HIsarna process was likely not optimized for such high CO_2 prices in the study of (Kuramochi et al., 2012), and the process could therefore probably be modified to further decrease its CO_2 intensity at a certain cost. This promising process is still undergoing pilot-scale demonstration and will require successful scale-up to become a commercial option (planned for 2030 (Tata Steel, 2020)). A detailed economic assessment of HIsarna and H_2-DRI using consistent methods and assumptions will be needed to assess the competitive positioning of these technologies with greater accuracy.

Finally, some mention can be made of the integration of blue hydrogen production from GSR (Nazir et al., 2020) or MA-ATR (Cloete et al., 2019) with the direct reduction shaft furnace. The most promising GSR integration would send the syngas from the GSR reforming step directly to the shaft furnace and use the low-grade fuel exiting the shaft furnace in the GSR reduction step to supply heat for the endothermic reforming. This is a configuration very similar to the commercial MIDREX process, only using the oxygen carrier in the GSR technology to inherently capture the CO_2 upon full combustion of the shaft furnace off-gases. When hydrogen is to be used directly in the shaft furnace, the MA-ATR process would be most attractive, given its excellent efficiency when supplying hydrogen close to atmospheric pressure. Both these routes would be able to capture almost 100% of produced CO_2 and enable the "Blue Optimistic" scenario in Figure S3. More detailed techno-economic assessments are recommended to accurately assess these promising integrations.

References

Agora, 2020. Making the Most of Offshore Wind: Re-Evaluating the Potential of Offshore Wind in the German North Sea. Agora Energiewende, Agora Verkehrswende, Technical University of Denmark and Max-Planck-Institute for Biogeochemistry.

Ahluwalia, R.K., Papadias, D.D., Peng, J.-K., Roh, H.S., 2019. System Level Analysis of Hydrogen Storage Options, in: Laboratory, A.N. (Ed.). US Department of Energy.

Amundsen, E.S., Bergman, L., 2006. Why has the Nordic electricity market worked so well? Utilities Policy 14, 148-157.

BP, 2020. Statistical review of world energy. British Petroleum.

Cloete, S., Khan, M.N., Amini, S., 2019. Economic assessment of membrane-assisted autothermal reforming for cost effective hydrogen production with CO2 capture. International Journal of Hydrogen Energy 44(7), 3492-3510.

Cloete, S., Ruhnau, O., Hirth, L., 2021. On capital utilization in the hydrogen economy: The quest to minimize idle capacity in renewables-rich energy systems. International Journal of Hydrogen Energy 46(1), 169-188.

EFN, 2021. Energy facts, Norway: Electricity production. https://energifaktanorge.no/en/norsk-energiforsyning/kraftproduksjon/ [accessed: 25/03/2021]).

Gorman, W., Mills, A., Wiser, R., 2019. Improving estimates of transmission capital costs for utility-scale wind and solar projects to inform renewable energy policy. Energy Policy 135, 110994.

IEA, 2019a. The future of hydrogen: Seizing today's opportunities. International Energy Agency.
IEA, 2019b. World Energy Outlook. International Energy Agency.
IEA, 2020. World Energy Outlook. International Energy Agency.
IEAGHG, 2011. The costs of CO2 transport: Post-demonstration CCS in the EU. European technology platform for zero emission fossil fuel power plants.
Kuramochi, T., Ramírez, A., Turkenburg, W., Faaij, A., 2012. Comparative assessment of CO2 capture technologies for carbon-intensive industrial processes. Progress in Energy and Combustion Science 38(1), 87-112.
LAK, 2021. Länderarbeitskreis (LAK) Energiebilanzen: Energie- und CO2-Bilanzen der Bundesländer. http://www.lak-energiebilanzen.de [accessed: 28/03/2021]).
May, T.W., Yeap, Y.M., Ukil, A., 2016. Comparative evaluation of power loss in HVAC and HVDC transmission systems, 2016 IEEE Region 10 Conference (TENCON). pp. 637-641.
Mongird, K., Viswanathan, V., Balducci, P., Alam, J., Fotedar, V., Koritarov, V., Hadjerioua, B., 2020. An Evaluation of Energy Storage Cost and Performance Characteristics. Energies 13(13), 3307.
Nazir, S.M., Cloete, J.H., Cloete, S., Amini, S., 2020. Pathways to low-cost clean hydrogen production with gas switching reforming. International Journal of Hydrogen Energy.
Neon, 2020. Open Power System Database. https://open-power-system-data.org/.
Norwegian Ministry of Petroleum and Energy, 2015. Facts - Energy and Water Resources in Norway.
NREL, 2018. Annual technology baseline. National Renewable Energy Laboratory. https://atb.nrel.gov/electricity/2018/index.html?t=cg [Accessed: 16.05.2021]).
NVE, 2020. Kostnader for kraftproduksjon. https://www.nve.no/energiforsyning/kraftmarkedsdata-og-analyser/kostnader-for-kraftproduksjon/ [accessed 12 November 2020]).
Pfenninger, S., Staffell, I., 2016. Long-term patterns of European PV output using 30 years of validated hourly reanalysis and satellite data. Energy 114, 1251-1265.
Staffell, I., Pfenninger, S., 2016. Using bias-corrected reanalysis to simulate current and future wind power output. Energy 114, 1224-1239.
Szima, S., Nazir, S.M., Cloete, S., Amini, S., Fogarasi, S., Cormos, A.-M., Cormos, C.-C., 2019. Gas switching reforming for flexible power and hydrogen production to balance variable renewables. Renewable and Sustainable Energy Reviews 110, 207-219.
Tata Steel, 2020. HIsarna - Building a sustainable steel industry. https://www.tatasteeleurope.com/ts/sites/default/files/TS%20Factsheet%20Hisarna%20ENG%20jan2020%20Vfinal03%204%20pag%20digital.pdf.
Vogl, V., Åhman, M., Nilsson, L.J., 2018. Assessment of hydrogen direct reduction for fossil-free steelmaking. Journal of Cleaner Production 203, 736-745.
Vrana, T.K., Härtel, P., 2018. Estimation of investment model cost parameters for VSC HVDC transmission infrastructure. Electric Power Systems Research 160, 99-108.
Walker, I., Madden, B., Tahir, F., 2018. Hydrogen supply chain evidence base. Elemental Energy.
Witkowski, A., Rusin, A., Majkut, M., Stolecka, K., 2017. Comprehensive analysis of hydrogen compression and pipeline transportation from thermodynamics and safety aspects. Energy 141, 2508-2518.